



**HAL**  
open science

## Actuation performance of embedded piezoceramic transducer in mechanically loaded composites

Christophe Paget, K. Levin, Christophe Delebarre

► **To cite this version:**

Christophe Paget, K. Levin, Christophe Delebarre. Actuation performance of embedded piezoceramic transducer in mechanically loaded composites. *Smart Materials and Structures*, 2002, 11 (6), pp.886-891. 10.1088/0964-1726/11/6/309 . hal-00149896

**HAL Id: hal-00149896**

**<https://hal.science/hal-00149896v1>**

Submitted on 19 Aug 2022

**HAL** is a multi-disciplinary open access archive for the deposit and dissemination of scientific research documents, whether they are published or not. The documents may come from teaching and research institutions in France or abroad, or from public or private research centers.

L'archive ouverte pluridisciplinaire **HAL**, est destinée au dépôt et à la diffusion de documents scientifiques de niveau recherche, publiés ou non, émanant des établissements d'enseignement et de recherche français ou étrangers, des laboratoires publics ou privés.



Distributed under a Creative Commons Attribution - NonCommercial 4.0 International License

# Actuation performance of embedded piezoceramic transducer in mechanically loaded composites

C A Paget<sup>1</sup>, K Levin<sup>1</sup> and C Delebarre<sup>2</sup>

<sup>1</sup> Aeronautics Division, Swedish Defence Research Agency, SE-172 90 Stockholm, Sweden

<sup>2</sup> IEMN (UMR CNRS 9929), Département OAE, Université de Valenciennes, Le Mont Houy, BP 311 F-59304 Valenciennes Cedex, France

## Abstract

The performance of embedded piezoceramic transducers (PZTs) used as Lamb wave generators was investigated in this paper. The composite specimens with a PZT embedded in the mid-plane were subjected to tensile and compressive monotonic loading as well as tension–compression fatigue loading. Both the static and fatigue tests revealed the large working range of embedded PZTs, despite the presence of damage observed by microscopy. The Lamb wave response remained unchanged after a large number of fatigue cycles; around 50 000–100 000 cycles at strain levels of  $\pm 0.20\%$ . At larger numbers of cycles, the changes in terms of amplitude and frequency in the Lamb wave response were believed to be associated with increasing matrix cracking in the specimens.

## 1. Introduction

Health monitoring using Lamb wave techniques [1] has been proposed to improve the safety and reduce maintenance in composite structures. Lamb waves can propagate in composites over long distances because of waveform conservation along the propagation path due to the non-dispersive nature of certain modes. Lamb waves, being a combination of several symmetric and anti-symmetric modes, may interfere with structural damage, resulting in changes in the features of specific modes, making it possible to detect damage [2, 3]. To process the Lamb wave response for damage detection, several methods are available, such as recognition of amplitude changes, Hilbert transforms and wavelet methods [2–5]. A method based on the group velocity of the Lamb waves enables damage to be located [6], and a Lamb wave technique was also tested for quantifying the damage extent [7] by recognizing the change in the amplitude of the power spectral density of the Lamb wave response. To improve the efficiency of such an active system in composites, piezoceramic transducers (PZTs) are embedded in the structure. The strength reduction in the composites due to the embedded PZT was found to be small [8] in a previous study.

Mall and Coleman [11] studied the influence of the tensile and fatigue mechanical loading on embedded PZTs

in quasi-isotropic carbon/epoxy composites. They showed that the transducers maintained a steady voltage output during mechanical cyclic loading at a strain limit of 0.15%. However, for higher strain levels, whether in tensile or fatigue tests, the transducer output voltage was degraded, probably due to a combination of depolarization, transducer deformation, grounding and damage modes of the composite specimens. Mall and Hsu [12] carried out tests on the performance of embedded PZTs in CFRP subjected to combined mechanical and electrical cyclic loading. The mechanical fatigue was achieved by loading the specimens up to 0.2% of strain with a stress ratio of 0.1. Simultaneously, the embedded transducers were electrically excited by two types of triangular waveform signal ranging from 10 to 100 V and  $-10$  to  $-100$  V, which resulted in out-of-phase and in-phase electrically induced strain, respectively. In out-of-phase condition, the fatigue life of the embedded PZTs was not reached after a million cycles for a strain level of 0.10%. At 0.17% of strain, the output signal of the transducers was degraded by 30% after about a million cycles. The same degradation of the transducer output signal was observed after 10 000 mechanical loading cycles with a strain level of 0.20%. In the case of the in-phase condition, the output signal of the embedded PZT was decreased by 30% after about 850 000 and 100 000 cycles at 0.10 and 0.17% of strain, respectively.

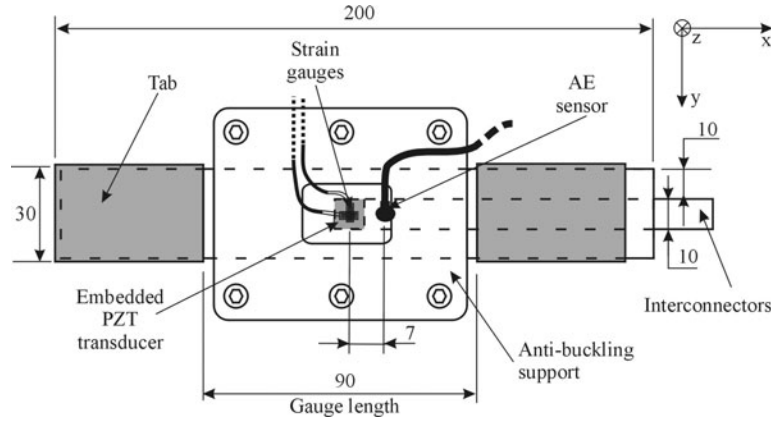


**Figure 1.** Specimen geometry (in mm).

The objective of this paper was to investigate the performance of embedded PZTs, using a similar approach to that of Mall and Hsu [12], but here with exposure to mechanical loading. However, this investigation focused on the ability of the transducers to generate Lamb waves in composites. The feasibility of using a concept based on embedded PZTs also relies on the fact that these must be durable over the entire structural life since no replacement is possible. The performance was determined by studying the generation of Lamb waves by embedded PZTs. The specimens were subjected to tension–compression fatigue loading as well as tensile and compression monotonic loading. The investigation of the PZT, as a Lamb wave generator, further focused on the changes of the amplitude and frequency in the Lamb wave response, based on the FFT and the envelope derivative of the Lamb wave response. Fractographic evaluation was performed to determine the critical part of the PZT in mechanical loading.

## 2. Specimen description

The transducer was made of a piezoceramic element with a pair of interconnectors. The transducer was approximately  $270 \mu\text{m}$  thick which was equivalent to two carbon/epoxy plies. The piezoceramic element (PZ-27 [9]) was 10 mm by 10 mm by 0.13 mm in size and was silver plated to improve the electrical conduction. The interconnectors were made of an  $18 \mu\text{m}$  thick copper layer bonded on a thin insulating polyimide film. The film was  $25 \mu\text{m}$  thick, and was 10 mm wide and 140 mm long. An approximately  $30 \mu\text{m}$  thick conductive adhesive was used to ensure both electrical conduction and a strong bonding between the piezoceramic element and the interconnectors.

The composite laminate for the present study was a cross-ply composite laminate,  $[0_4/90_4/0_4/90_4/0_2/\{\text{PZT}\}]_S$ , made of carbon fibre-reinforced epoxy (HTA/6376C). The PZT was embedded in the mid-plane of the laminate. The laminate was cured in an autoclave at  $180^\circ\text{C}$ . The laminate thickness was 4.79 mm. The composite plate was further cut into specimens with dimensions of 200 mm by 30 mm, as shown in figure 1. Steel tabs were bonded to the specimen with a high-strength epoxy adhesive (FM 300) to avoid premature failure.

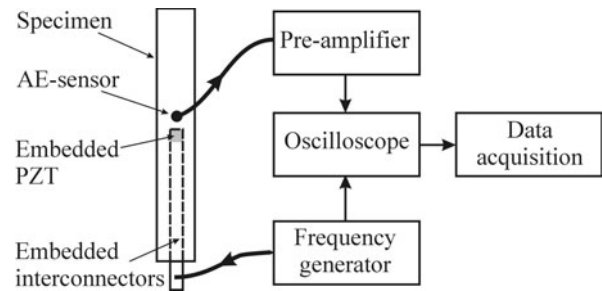


**Figure 2.** The experimental set-up for the Lamb wave generation.

## 3. Test procedure

The experimental set-up for the generation of Lamb waves in composites is shown in figure 2. A 250 kN servo-hydraulic testing machine was used for the mechanical testing in static and fatigue loading. Aluminium plates, which were 15 mm thick, were used as anti-buckling support in static compression and fatigue loading. The anti-buckling plates had a 30 mm by 24 mm opening in the centre, and were placed at the gauge section as shown in figure 1. The friction between the specimen and the anti-buckling plates was minimized using a film of PTFE (Teflon).

A frequency generator was used to power the PZT, generating a rectangular-windowed five-cycle sinusoidal tone burst. The input signal frequency was 130 kHz. A surface-attached acoustic emission (AE) sensor, which detected the response, was located about 7 mm from the centre of the PZT, as shown in figure 1. A pre-amplifier was necessary to both amplify the AE sensor signal by 40 dB and filter the signal noise by a built-in low-pass filter. A digital oscilloscope (LeCroy 300 MHz) was used to collect the data from the AE sensor, further retrieved by computer via a GPIB bus for data analysis. The oscilloscope monitored the Lamb wave response by collecting every single shot triggered by the tone burst from the frequency generator. The sample rate was  $1 \text{ Ms}^{-1}$ . As an effect of the storage capacity of the oscilloscope, the tone bursts were generated every 8 s in tension and every 5 s in compression, owing to higher load in tension. Therefore the tone burst occurred at loading increments of 56 and 36 MPa in tension and compression, respectively.

Eight and six specimens were tested in tensile and compressive monotonic loading, respectively. In fatigue, 15 specimens were tested at four different stress levels; at least three specimens per stress level. For the specimens statically loaded, the loading rate was  $1 \text{ kN s}^{-1}$  corresponding to an increase in the applied stress of about  $7 \text{ MPa s}^{-1}$ , and in the fatigue tests the loading frequency was  $1 \text{ Hz}$ . In fatigue loading, all the specimens were subjected to load-controlled, tension–compression conditions with the stress ratio (ratio of minimum stress to maximum stress)  $R = -1$ . The measurements were performed in the unloaded condition after 1, 5, 10, 50, 100 etc cycles. The testing was however stopped at  $4 \times 10^5$  cycles. In addition, the Lamb wave response before the first cycle was considered as the reference signal for the analysis.

Because of the specimen edges, the Lamb wave response included reflections of the Lamb wave modes [2]. The first Lamb mode collected by the AE sensor was the  $S_0$  mode, direct, since this mode propagated with the fastest velocity, which is in the present case  $7 \text{ km s}^{-1}$ . However, it was impossible to distinguish the  $S_0$  mode, direct, from its reflections since the waveform duration of this mode ( $38 \mu\text{s}$ ) was larger than the time of flight of the  $S_0$ -mode reflections. Any damage at the edges of the loaded specimens was expected to change the Lamb wave response collected by the AE sensor. Consequently, the specimen edges were carefully checked during the course of the experiments to monitor any edge damage initiation that could interfere with the resulting analysis of the Lamb wave response.

In static tests, the AE sensors were surface bonded to the specimens by silicone paste. However, in the fatigue tests, no coupling agents were used to avoid the effect of degraded coupling properties throughout the large numbers of fatigue cycles. The AE sensors were therefore directly fixed on the specimen surface.

#### 4. Results

The performance of embedded PZTs used as Lamb wave generators was studied. The study was mainly based on the changes in the amplitude and frequency spectrum of the Lamb wave response, to detect any degradation or loss in the generation of Lamb waves due to mechanical loading. Therefore in the static and fatigue tests, the FFT modulus of the Lamb wave response was used:

$$|\text{FFT}| = 10 \log_{10}(\text{Re}(\text{FFT})^2 + \text{Im}(\text{FFT})^2). \quad (1)$$

However, in fatigue tests, no coupling agent was used, and friction between the AE sensor and the specimen may interfere in the FFT magnitude of the Lamb wave response. Therefore, another technique was used to complement the results obtained with the FFT-based technique. This second technique, known as the *time difference parameter* (TDP) technique, allows the processing of complex Lamb wave responses,  $x(t)$ , such as those dealt herein [10]. The technique uses the envelope of the Lamb wave response, defined as

$$\check{x}(t) = \sqrt{x(t)^2 + H[x(t)]^2}, \quad (2)$$

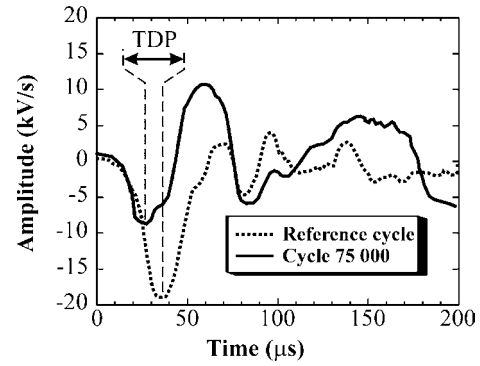


**Figure 3.** An example of an envelope derivative of the Lamb wave response at  $\pm 0.3\%$  strain and at cycles 0, 75 000.

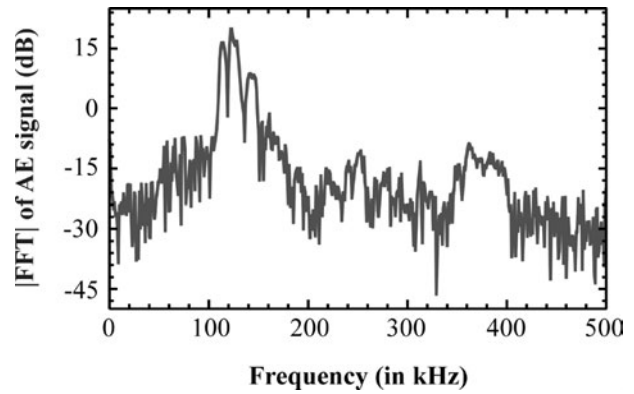


**Figure 4.** The FFT modulus of a typical Lamb wave response.

where  $x(t)$  is the Lamb wave response and  $H[x(t)]$  its Hilbert transform. The Hilbert transform is defined by the following equation:

$$H[x(t)] = \frac{1}{\pi} \int_{-\infty}^{+\infty} \frac{x(\tau)}{t - \tau} d\tau. \quad (3)$$

The TDP technique further uses the envelope derivative of the Lamb wave response,  $\frac{dx}{dt}$ . The TDP corresponds to the time separating the first minima of the two envelope derivatives, which are at the reference cycle (before loading) and at a specified cycle, as shown in figure 3.

##### 4.1. Monotonic loading

The performance of the embedded PZT as a Lamb wave generator was evaluated. The Lamb wave response collected by the AE sensor was monitored during tension and compression monotonic loading in order to detect anomalies related to degradation of the transducer performance. The amplitude and frequency of the FFT modulus of the Lamb wave response were used to monitor changes in the Lamb wave response. Figure 4 represents an FFT example of a Lamb wave response. It consisted of a signal with frequencies inside the range 100–200 kHz, centred on 130 kHz which was imposed by the excitation signal of the Lamb wave generator. The analysis of the Lamb wave response showed similar responses throughout the monotonic loading, and up to large strain levels, despite the increasing stresses applied to the embedded PZT during loading.

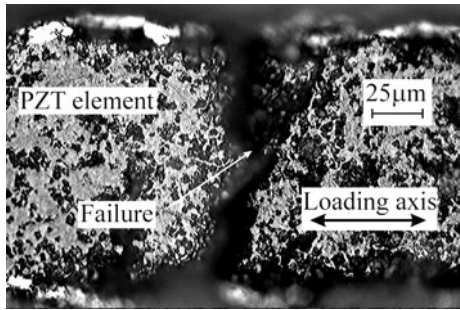


**Figure 5.** Failure in the piezoceramic element in tension.

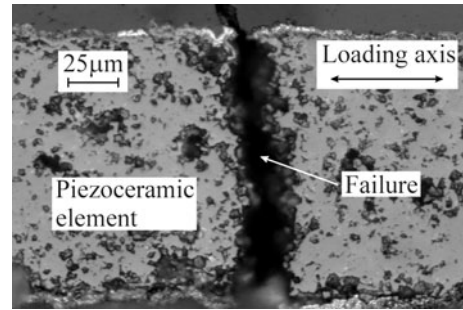


**Figure 7.** Failure in the piezoceramic element in compression.

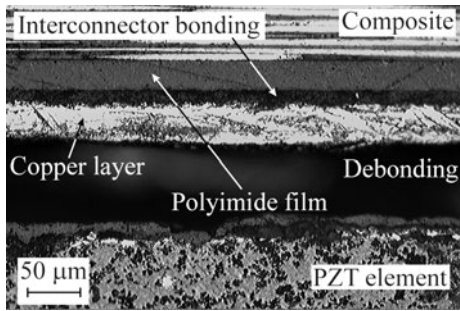


**Figure 6.** Damage of the bond between the interconnector and piezoceramic element in tension tests.

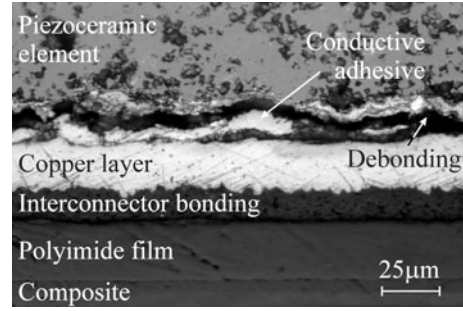


**Figure 8.** Debonding between the conductive adhesive and piezoceramic element in compression tests.

In tensile tests, the last recorded response did not show significant changes. This response corresponded to a Lamb wave response at 90% of the final failure load limited by the storage capacity of the measurement system. However, the PZT still functioned after the final failure of the tensile specimens. The fractographic examination was performed on specimens loaded close to failure (about 1 GPa) in order to avoid other damage caused by the energy released from the final failure. Fractographic evaluation of those specimens showed the presence of matrix cracks in the 90° plies.

However, those matrix cracks could not be detected by the active damage detection system, based on an embedded PZT and an AE sensor. This was due to the wavelengths of the Lamb wave modes propagating in the composite (11 and 54 mm [3]), which were far larger than the size of the matrix cracks. Also, failures in the piezoceramic element and damage of the bond between the piezoceramic element and the interconnector were observed, as shown in figures 5 and 6.

In compression, the PZT functioned properly at least up to  $\approx 95\%$  of the failure load. At this load level the contact with the surface-attached AE sensor was usually lost. As a result, it was not possible to determine whether the performance of the transducer was degraded above this load level. The damage in compression-loaded specimens involved several failure mechanisms in the region of the embedded PZT, such as debonding of the interface between the piezoceramic element and the adhesive as well as failure in the piezoceramic element, as shown in figures 7 and 8. Matrix cracks and fibre breakage were also noticed, but these damage mechanisms were probably a result of the final failure.

This study with this particular detection technique demonstrated that monitoring of composites during monotonic loading was not suitable for detecting matrix cracks. In the

same way, this detection technique was not able to self-monitor, since failures in the piezoceramic element and damage of the bond between the piezoceramic element and the interconnector could not be identified. The next section therefore does not involve monitoring during loading.

#### 4.2. Fatigue loading

The modulus of the FFT of the detected Lamb wave response before loading was compared with the modulus of the FFT of the Lamb wave response at specified cycles. The measurements were performed after reaching those loading cycles and also at zero loads since the static tests proved deficient, for example in detecting matrix cracks using continuous monitoring. After every specified cycle number, changes in terms of amplitude and frequency of the FFT modulus of the Lamb wave response were investigated. The second technique, called the TDP technique, was also used to verify those results, as shown in figure 9. The results are summarized in table 1 for all specimens loaded in fatigue. Those results coincided with those obtained with the FFT magnitude technique.

At stress levels up to  $\pm 130$  MPa, corresponding to  $\pm 0.15\%$  of strain, no significant changes in the Lamb wave response in terms of frequency and amplitude were observed after 400 000 loading cycles, as shown in figure 9. In the specimens loaded at  $\pm 170$  MPa, corresponding to  $\pm 0.20\%$  of strain, a slight decrease in the amplitude of the FFT was noticed at around 50 000–100 000 cycles. At  $\pm 260$  MPa, corresponding to  $\pm 0.30\%$  of strain, a significant degradation of the Lamb wave generation was noticed at 50 000–100 000 loading cycles, as shown in figures 9 and 10.

Fractographic examination of the specimens loaded up to  $\pm 130$  MPa did not reveal any damage in the composite

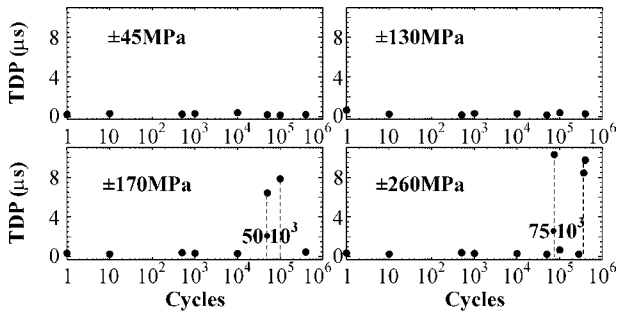


**Figure 9.** TDPs of specimens loaded up to  $4 \times 10^5$  cycles at four different stress levels.

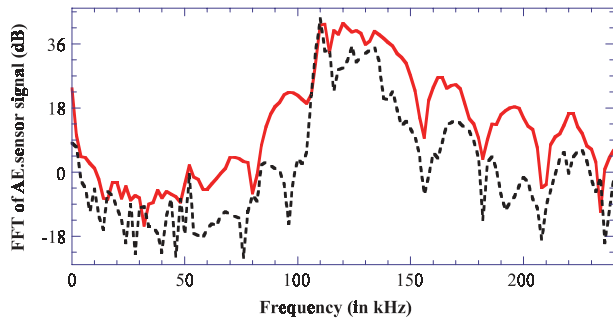


**Figure 10.** The FFT modulus of the Lamb wave response at 100 000 cycles (dashed curve) and the reference cycle (solid curve) of specimen FA10.

(This figure is in colour only in the electronic version)

**Table 1.** Detected changes of the Lamb wave response in fatigue tests.

Specimen name	Stress level (MPa)	Cycle range where changes occurred	Changes in the modulus of FFTs
FA1-3	$\pm 45$	None	No significant changes
FA4-7	$\pm 130$	None	No significant changes
FA8-12	$\pm 170$	50 000–100 000	Slight decrease in amplitude
FA13-15	$\pm 260$	50 000–100 000	Significantly attenuated

or the embedded PZT. In the specimens loaded in fatigue at  $\pm 170$  MPa, matrix cracks appeared in the region of the AE sensor and the PZT between 100 000 and 400 000 loading cycles. The first failures in the PZT appeared before 50 000 cycles. The fractographic examination also showed debonding between the conductive adhesive and the piezoceramic element in various locations after 100 000 cycles. The same damage mechanisms as for the specimens loaded at  $\pm 170$  MPa were observed in the specimens loaded to  $\pm 260$  MPa. The damage, shown in figures 11 and 12, occurred at similar loading cycles but with a larger number of matrix cracks and PZT failures. These observations indicate that damage can have a significant effect on the performance of the transducer in fatigue loading. The debonding between the conductive adhesive and the piezoceramic element was observed at an earlier stage than for specimens loaded at  $\pm 170$  MPa, that is before 40 000 cy-

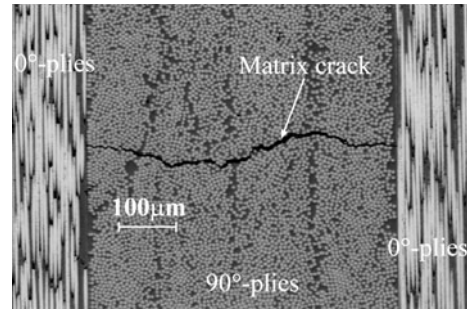


**Figure 11.** A matrix crack in a  $90^\circ$  ply in a fatigue-loaded specimen at  $\pm 260$  MPa.

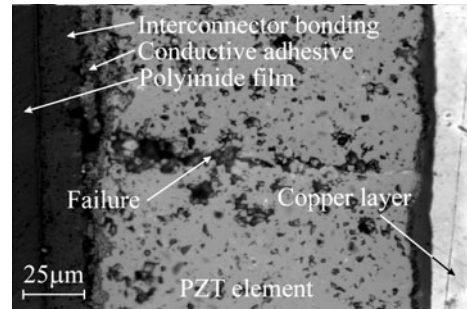


**Figure 12.** Piezoceramic failure in a specimen loaded in fatigue at  $\pm 260$  MPa.

cles. At 400 000 cycles the debonding was more extensive in the  $\pm 260$  MPa specimens. However, it appears that the debonding in the embedded PZT did not significantly affect the generation of Lamb waves, as also observed in the static tests. Therefore the changes detected in the Lamb wave response were perhaps related to the presence of matrix cracks. This phenomenon was not identified in the static tests.

## 5. Conclusions

The embedded PZTs revealed a large working range in the static tests at least up to 90% of the final failure. The embedded PZTs were found to be insignificantly affected by fatigue loading. For low stress levels, below 0.20% of strain, the PZT had a high working range, more than 400 000 cycles. Changes in the Lamb wave response only occurred after a large number of cycles at high stress levels. The results showed that any damage occurring at the transducer location did not affect the transducer performance in either static or fatigue loading. The transducer could therefore function even after the occurrence of the damage.

## Acknowledgments

The authors acknowledge FMV (The Defence Material Administration) and FOI (The Aeronautics Division of The Swedish Defence Research Agency) for financial support. Lennart Nystedt and Bengt Wallstenius, at FOI, are thanked for their help during the experiments and Dr Arne Skontorp, also at FOI, for his comments on the manuscript. Dr Sébastien Grondel at IEMN (The Microelectronics and Electronics Institute of Northern France) is also acknowledged for fruitful discussions during the course of this work.

## References

- [1] Okafor A C, Chandrashekhara K, Jiang Y P and Kilcher R R 1994 Damage assessment of smart composite plates using piezoceramic and acoustic emission sensors *SPIE Proc.* **2191** 265–75
- [2] Paget C A 1998 Feasibility of an active system to detect impact damage in a composite panel by Lamb waves propagation—preliminary evaluation *Swedish Defence Research Agency Technical Report* FFAP H-1356
- [3] Paget C A 2001 Contribution to active health monitoring of aerospace structures by embedded piezoceramic transducers *PhD Thesis* 0117, Valenciennes University
- [4] Okafor A C, Chandrashekhara K and Jiang Y P 1995 Damage detection in composite laminates with built-in piezoelectric devices using modal analysis and neural network *SPIE Proc.* **2444** 314–25
- [5] Choi K, Keilers Jr C H and Chang F-K 1994 Impact damage detection in composite structures using distributed piezoceramics *Proc. AIAA Conf. on Structures, Structural Dynamics and Materials Part I, 94-1322* (Reston, VA: AIAA) pp 118–24
- [6] Shen B S, Tracy M, Roh Y-S and Chang F-K 1996 Built-in piezoelectrics for processing and health monitoring of composite structures *J. AIAA* **1310** 390–7
- [7] Blanquet P 1997 Etude de l'endommagement des matériaux composites aéronautiques à partir des techniques ultrasonores *PhD Thesis* Valenciennes University
- [8] Paget C A and Levin K 1999 Structural integrity of composites with embedded piezoelectric ceramic transducer *SPIE Proc.* **3668** 306–13
- [9] *Data Sheet for Piezoceramic Element PZ-27* Ferroperm, Piezoceramic division, Hejreskovvej 6, 3490 Kvistgård, Denmark
- [10] Grondel S, Delebarre C, Assaad J, Dupuis J-P and Reithler L 2001 Fatigue crack monitoring of riveted aluminium strap joints by Lamb wave analysis and acoustic emission measurement techniques *NDT&E Int.* **35** 137–46
- [11] Mall S and Coleman J M 1998 Monotonic and fatigue loading behaviour of quasi-isotropic graphite/epoxy laminate embedded with piezoelectric sensor *Smart Mater. Struct.* **7** 822–32
- [12] Mall S and Hsu T L 2000 Electromechanical fatigue behaviour of graphite/epoxy laminate embedded with piezoelectric actuator *Smart Mater. Struct.* **9** 78–84